A biophysical model for curvature-guided cell migration

Maxime Vassaux, Laurent Pieuchot, Karine Anselme, Maxence Bigerelle, Jean-Louis Milan

Manuscript submitted to **Biophysical***Journal*
Article

A biophysical model for curvature-guided cell migration

Maxime Vassaux[1,2,*], Laurent Pieuchot[3,4,*], Karine Anselme[3,4], Maxence Bigerelle[5], and Jean-Louis Milan[1,2]

[1]Institute of Movement Sciences, Aix Marseille University, CNRS, Marseille, France
[2]Department of Orthopaedics and Traumatology, Institute for Locomotion, APHM, Sainte-Marguerite Hospital, Marseille, France
[3]Université de Haute-Alsace, CNRS, IS2M, UMR 7361, Mulhouse, F-68100, France
[4]Université de Strasbourg, Strasbourg, F-67081, France
[5]Université de Valenciennes et du Hainaut Cambrésis, Laboratoire d'Automatique, de Mécanique et d'Informatique industrielle et Humaine (LAMIH), UMR-CNRS 8201, Le Mont Houy, Valenciennes, France
[*]Correspondence: laurent.pieuchot@uha.fr, m.vassaux@ucl.ac.uk

ABSTRACT Latest experiments have shown that adherent cells can migrate according to cell-scale curvature variations via a process called curvotaxis. Despite identification of key cellular factors, a clear understanding of the mechanism is lacking. We employ a mechanical model featuring a detailed description of the cytoskeleton filament networks, the viscous cytosol, the cell adhesion dynamics and the nucleus. We simulate cell adhesion and migration on sinusoidal substrates. We show that cell adhesion on three-dimensional curvatures induces a gradient of pressure inside the cell that triggers the internal motion of the nucleus. We propose that the resulting out-of-equilibrium position of the nucleus alters cell migration directionality, leading to cell motility toward concave regions of the substrate, resulting in lower potential energy states. Altogether, we propose a simple mechanism explaining how intracellular mechanics enable the cells to react to substratum curvature, induce a deterministic cell polarization and breakdown cells basic persistent random walk, which correlates with latest experimental evidences.

INTRODUCTION

Adhesion and migration are central processes in physiological cellular activities depending on the interaction between the cell and the extracellular matrix or biomaterial surfaces (1–3). The current paradigm is that biochemistry controls adhesion and migration. Nonetheless, mechanical properties of the substrate also influence adhesion, hence controlling spreading area and intracellular tension. As such, mechanobiology tells us that adhesion and migration, if controlled and understood, can provide a way to manipulate cell fate (4, 5) and avoid severe pathologies (6). Recent findings in cell mechanobiology have shown the correlation between the mechanical state perceived by the cell and, how it differentiates, proliferates, and dies (7–10). Designing efficient technologies to manipulate cells fate relies partly on understanding the mechanisms triggered by the complex combination of mechanical cues induced by their surrounding environment (11, 12). Unravelling the interaction between substrate topography and cell behaviour is therefore of the utmost significance (3, 13).

Multiples environmental factors wield cell migration, and related processes. Earliest discoveries related the influence of chemical and ligand gradients on the substrate, and respectively coined the names *chemotaxis*(14) and *haptotaxis*(2, 6). More recent findings showed that cell migration is also directed by purely mechanical cues, such as stiffness gradients (*durotaxis*) (15), topographic pattern gradients (*topotaxis*) (16) and substrate anisotropy (*ratchetaxis*) (17–19). Lastly, microscopic curved topographies have gained greater interest for their resemblance with smooth biological tissues (20–23). A recurrent factor in these directed migration mechanisms is the predominant role of the nucleus (24, 25). Nucleus mechanosensitivity, defined as the interplay between nuclear mechanics and regulation of gene expression, has recently drawn further attention for its influence on a wide array of physiological behaviour (26, 27). Ratchetaxis is shown to depend on the polarization of the nucleus and its interplay with stress fibers (18). On curved topographies, the mechanical stress of the nucleus is directly correlated with the curvature of the substrate (21, 28).

In a recent study, we have shown that adherent cells are able to migrate according to curvature variations via a process called "curvotaxis" Pieuchot et al. (29). Trajectories of cell migration on three-dimensional sinusoids revealed systematic circumvention of convex topographies and the positioning of cells on concave minima. Functional assays suggest that the mechanism requires actomyosin contractility, high nuclear lamin A levels and functional LINC complexes. In turn, we proposed that the short-range mechanosensitivity of the nucleus, mechanically interacting with the cytoskeleton, was proposed to play a central role in curvature-directed cell migration. However, a mechanistic model explaining the cellular and mechanical basis of curvotaxis was lacking.

Retrieving data *in vivo* or *in vitro* at the sub-micron scale is hampered by the size and the dynamics of the structures to investigate. In turn, *in silico* systems reveal a complementary approach to obtain insights in the mechanics of the structural components of cells (30). Computational models of single cell mechanics are scarce. The collective dynamics of the nucleus, the cytoskeleton and the membrane of the cell cannot be integrated using methods deriving from molecular dynamics within reasonable computational costs (31). In the meantime, higher-level methods, such as Cellular Potts (32–34) or random walk (35) models are too coarse to permit the investigation of internal cell mechanics. An intermediate approach based on particles and springs has proven efficient to capture the mechanical specificity of the cytosol, the cytoskeleton and the nucleus while integrating environmental cues (36–38). The primary components of the cell model are a fluid cytosol, a solid assembly of beams and cables that mimic the cytoskeleton, and a elastic nucleus. Furthermore, such approach integrates the contractile behaviour of the stress fibers and the actin cortex. As such, mechanical stability of the cell model arises from the osmotic pressure inside the cytosol and the structural rigidity of the cytoskeleton. With such level of detail, particle-based models are ideal tools to explore the reorganization of the cytoskeleton and the nucleus under external mechanical cues, that is substrate topography.

Here, we exploit the capabilities of a validated mechanical cell model (28) to provide insights into the mechanism of curvature-guided cell migration. We simulate cell adhesion on different locations of a 3D sinusoid and, observe non-equilibrium mechanics of the cytoskeleton and internal motions of the nucleus. We establish a back-and-forth comparison between our computational predictions and the experimental data. Finally, we propose a cell migration mechanism based on internal motion and polarization of the nucleus.

METHODS

The simulations of adhesion and migration of cells on sinusoid substrates are a direct application of the model proposed by Vassaux and Milan (28) based on the LMGC90 software (39). The structure of the cell is depicted as an assembly of rigid particles subject to Newton's equation of motion and interacting via an harmonic potential (40–42). Such modelling method, very similar to coarse-grained molecular dynamics or bead-spring models, accurately reproduces the discrete structures of biological systems, from proteins and DNA (43, 44) to cells and packing of cells (45, 46). The cell basically consists of an elastic impermeable membrane encapsulating a viscous cytosol and a deformable nucleus. In addition, the cytoskeleton is introduced as a dynamic assembly of competing compressive and contractile networks (45, 47, 48).

Our model explicitly integrates actin, microtubules and intermediate filaments networks, contractile stress fibres, a contractile actomyosin cortex mingled in the cytoplasmic membrane, a viscous cytosol and a viscoplastic nucleus (see figure S3.b). The parameterization of the model's interaction potentials (see figure S3.a) has been largely verified and validated against indentation tests Vassaux and Milan (28). Complete details on the mathematical foundation of the model as well as the calibration, validation and adhesion simulation process can be found in the Supplementary Material. This mechanical cell model is able to capture realistic nucleus dynamics (see figure S3.f), that is nucleus equilibrium on a flat topography is found at the center of the cell. These are governed by the coupled contribution of viscous, inertial (nucleus mass), and elastoplastic (conformational changes in the cytoskeleton) effects. Atomic force microscopy indentation experiments on endothelial and Schwann cells (27) reveal that vertical forces on the nucleus can cause its internal sliding, and the subsequent existence of such pulling back forces ensuring its centered position.

Simulations of cell adhesion all follow the same procedure. In their initial configuration, the simulated cells display a spherical shape. We consider 3 diameters of cell: 20, 30 and 50μm associated respectively with the diameters of nucleus: 10, 20 and 30μm. Spreading is actioned following the displacement of the focal adhesions (FAs) away from the center of cell, following the topography of the substrate. The diameters of adhered cells approximate 60, 100, 150 ~~35~~μm diameter, respectively. This dynamic adhesion process, coupled with actomyosin contraction in stress fibers and the actin network, induces conformational changes in the cytoskeleton. At the end of the simulation, cells are pulled onto the substrate and attached via 30 focal points. Focal adhesions are distributed at cell's periphery - in a 25μm wide band for a 100μm diameter adherent cell - and this, regardless of the site of the cell adhesion in a concave, convex or in the transitional areas.

Subsequently, the adhesion model has been extended to render migration tractable. The migration is simulated by reproducing in a simplified way the simultaneous protrusion of a lamellipodium at the front and the cell retraction at the back of the cell. The cell model migrates as new focal adhesions are continuously assembled away from existing disassembling adhesions, in the direction of motion. While the cytoskeleton connects the new focal adhesions, the old ones are disassembled. We hypothesized that the lamellipodium forms in the direction of the topography-induced polarization of the nucleus and advances proportionally to nucleus internal motion. The internal displacement of the nucleus $\underline{d}$ is computed as the vector directed from the cell barycenter to the nucleus barycenter. The spatial jump $\underline{v}^t$ (amplitude, direction) from the disassembled adhesions to the assembled ones at time t, is equal to the internal displacement of the nucleus $\underline{d}^{t-1}$, observed at time $t-1$. The simulation of cell migration ends when $\underline{d}^t$ becomes negligible with respect to the cell dimensions, that is when the cell is assumed to have

Figure 1: **Triggering the nucleus motion.** (a) Tracking of nuclei motions (dashed lines) with fixed cell adhesions on a map of the sinusoid (the initial position of the nuclei is denoted by a black cross, which is also the center of the immobile cell) in the horizontal plane. Simulation of 100μm cell adhering on 10-100μm sinusoid. Colored squares refer to the pressure maps of the respective cells. (b, d-g) Maps of the vertical pressure distributions under the cell on the substrate. Arrows show the instant amplitude and direction of motion of the nuclei. On uneven substrates b, d, e the nuclei move away from the high-pressure areas, while on the top of convex or at the bottom of concave the pressure is homogeneous and the nuclei barely move. (c) Side view of the cell, nucleus and cytoplasmic membrane, in b showing motion from the top of the convex to the bottom of the concave. (h, i) Three-dimensional view of the nuclei found respectively on (h) a convex (f) and (i) a concave (g), one is round, the other is stretched. The particles, constituting the nucleus membrane, are colored as a function of the local cohesion forces amplitude.

stabilized. Such procedure renders a continuous migration of the cell (see animation S1).

In more details, at the beginning of simulation, at time step 0, the cell model is spread and adheres to the sinusoidal substrate at a given location and the displacement of the nucleus is reported after cell spreading as a vector $\underline{d}^0$, the spatial jump $\underline{v}^0$ is null. Next, at the time step 1, the cell model migrates on the sinusoidal surface, as the lamellipodium progresses, and stops when the new focal adhesions are remote from the disassembled ones by $\underline{v}^1 = \underline{d}^0$. The new internal offset of the nucleus is reported as $\underline{d}^1$. In the following time steps, the procedure is repeated with $\underline{v}^t = \underline{d}^{t-1}$.

With these cell adhesion and migration models in hand, the computational campaign is performed in two parts. First, we simulate the adhesion of 26 cells position at regular distance intervals within a wavelength of the sinusoid. The tested sinusoid has an min-to-max amplitude of 10 μm and a wavelength of 100~~30~~ μm, so called the 10-100μm sinusoid. Second, we simulate the complete migration of 5 of these cells, using the proposed model. The retained cells are chosen in order to investigate the influence of a varied array of initial topographies. We analyze the influence of sinusoid sizes on cell migration in considering the following couples of amplitude-wavelength: 3-30μm, 10-30μm, 30-100μm, 30-300μm.

RESULTS AND DISCUSSIONS

Several cells, structurally identical, are left to adhere in different locations (crosses, see figure 1.a). We observe the motion of the nuclei center (dashed lines, see figure 1.a). Since the cell is fixed at the focal adhesions, we in fact observe the internal displacement of the nucleus in the cytoplasm.

The nucleus is initially centered in the cell membrane, but within microseconds starts to drift along the substrate topography. Internal displacement is systematically observed, except for three nuclei: one positioned on top of a convex (purple square, see figure 1.a), one positioned at the bottom of a concave (yellow square, see figure 1.a), and one positioned on a saddle point of the sinusoid. In all other cells, the nucleus moves towards lower heights, which also correspond to locations of concave curvatures. Experimental findings by Pieuchot et al. (29) show identical trends, the nuclei stabilizing in concave regions (see figure S4.a,d). The magnitude of the displacement of the nuclei correlates strongly with the degree of anisotropy of the underlying topography, at scales perceived by the cell. Indeed, the three cells whose nucleus stands still interact with a symmetrical substrate topography. The simulations also tend to show that the nuclei follow the steepest gradients trajectories. Although, this displacement is directed toward lower parts of the substrate, the influence of the gravitational field is insignificant. This is shown experimentally by Pieuchot et al. (29) and computationally, inverting the direction of the gravity field. Furthermore, we have computed the resulting pressure applied by the cells on the substrate (see figures 1.b,d,e,f,g). On axial symmetrical topographies, namely convex peaks and concave valleys, the pressure is isotropically distributed around the nucleus (see figure 1.f,g). On the contrary, when the symmetry of the underlying substrate topography is broken, a pressure gradient appears on the substrate, and therefore in the cytoskeleton (see figure 1.b,d,e).

The morphology of the nucleus drastically changes with the underlying topography. As the cell migrates across the substrate, the nucleus can be elongated on convex regions, and round on concaves (see respectively figures 2.h and 2.i). The similar observation is made experimentally (see figure S4.g,h) which confirms the mechanics reproduced by the model. It is interesting to observe that topography directly impacts nucleus shape, that is known to regulate gene expression. Indeed, nucleus shape controls condensation of chromatin, and therefore which genes are exposed for transcription (49). Nucleus shape also controls nucleopores width. Nucleopores are enlarged when the nucleus stretches, which is known to increase transport rate of proteins, such as transcription factors, inside the nucleus (50). In turn, cells position on a sinusoid can be seen alternatively as a positive or negative regulation mechanism, whether it is located on a convex or a concave.

Simulations of cell adhesion on these different topographies show that motion of the nuclei is triggered by the spreading of the cells on the uneven, asymmetric substrate topography. As the cell spreads, its actin cortex is stretched which increases the vertical pressure inside the cell, and more specifically on the nucleus. The anisotropy of the underlying topography yields a

Figure 2: **Nucleus motion guided migration.** (a) Comparison of the nucleus centering mechanism induced either by pulling back up the nucleus or by a repositioning of the membrane. (b) Tracking of cells barycenter motions with nucleus-guided migrating cell adhesions on a map of the sinusoid. Simulation of 100μm cells migrating on 10-100μm sinusoid. The size and darkness of the circles illustrates the vertical stress inside the nuclei. The circles and black dots are snapshots are regular time intervals. The five cells studied are the same cells observed in details in the figure 1. White crosses denote the initial position of the cells. (c) Time evolution of the nuclei vertical pressure in green and of the speed of the cells in blue. Frames are associated to the cells of identical color on the map (b).

Figure 3: **Cortical tension and nuclear stiffness control cell migration.** The cell (a,b) adhesion and (c) migration simulations are performed again, this time with altered parameters. Essentially, the influence of a modified (a-right, c) contractility of the cytoplasmic membrane actomyosin cortex, or (a-left) stiffness of the nucleus is observed. (a,b) In adhesions simulations, the contractility and the stiffness are multiplied by 0.1, 0.05 and 0.02 and checked against control (original parameter set). (b) Quantification of the actual internal displacement of the nucleus show a strong dependence to both parameters. Conversely, the shape of the cell does not alter the mechanosensitivity of the nucleus. (c) In migration simulation, only the influence of the cortical tension is tested, by reducing it 10-fold. (d) As the pressure on the nucleus drastically reduces with lower actin cortex tension, the migration velocity drops down.

pressure gradient inside the cytoskeleton, pushing the nucleus out of equilibrium. A flow results inside the cytosol, moving matter from high to low pressure areas. Finally, the motion of the nuclei can only be stopped when recovering an homogeneous internal pressure, that is to say, the symmetry of the underlying substrate. Complementary simulations performed reducing either the nucleus stiffness or the cytoplasmic membrane actomyosin cortex (that encompasses stress fibres) tension show drastically impeded nucleus internal motion (see figure 3.a,b). As a result, such mechanism consistently explains the internal motion of the nuclei from parts of the cell located over convex topographical areas to concave ones (see figure 1.c).

We establish the hypothesis that the migration of the cell is induced by the polarized position of the nucleus. This hypothesis is based on our previous *in vitro* results by Pieuchot et al. (29). Indeed, the precedence of nuclear motion in the migration process on curved topographies has been observed experimentally (see figure S4.e,f). In response, to restore mechanical equilibrium and stability, the nucleus need to be centered again. Studies have highlighted the importance of the distance in between the nucleus and the cell center for polarization and division processes (51). Repositioning of the nucleus could be achieved by the cell through several mechanisms involving actin (52), or microtubules pulling on the cell membrane (53, 54). Two main mechanisms can be isolated: (i) pulling and squeezing the nucleus back up the slope, with fixed cell adhesions, opposing the pressure exerted by the stretched actin cortex (left case, see figure 2.a), and (ii) deconstruction and reconstruction of the cell adhesions down the slope, which would relax the actin cortex, while dynamically deactivating and reactivating the focal adhesions (right case, see figure 2.b). Both recruit different quantities of energy. The latter induces relaxation of the cell and nucleus membranes, and therefore, may require the cell to recruit less mechanical energy. That is an experimentally known precursor to cell migration (55). In the other scenario, forcing the repositioning of the nucleus at the centre of the cell drastically increases its vertical stress (see figure S3.g). What's more, the work required to displace identically the nucleus is higher than on a flat surface (see figure S3.f). Besides, the concave topography constitutes a well, that is a mechanically more stable position for the nucleus.

We now address the simulation of cell migration on the sinusoid substrate. The assumption of a nucleus-guided cell migration is implemented (see Methods section) and now tested. The offset in between the nucleus barycenter and the adhesions barycenter is evaluated at regular time intervals and converted into lamellipodium protrusion and spatial jump from the disassembled adhesions to the assembled ones. For these simulations, only the five cells studied in details in figure 1 are considered (see figure 2.b,c). Our simulations successfully reproduced the experimental migration trajectories (see figure S4.c,d). In all five cases, the cells migrate downward along the slopes, and stabilize at the bottom of concaves (see figure 2.b). Taking the case shown in cyan color in figure 2.b as a reference, we simulated cell migration in varying cell size and substrate curvature. Results shows that curvotaxis is better if sinsuoid wavelength is similar to cell size (see figures 4 & 5). Indeed, in this case, the concave zone offers the greatest relaxation volume to which the nucleus can move and guide the cell migration. Nonetheless, on 10-100 μm sinusoid, the simulation shows that the curvotaxis is better in terms of trajectory and speed for 150 μm adherent rather than for the 100 μm cell. We can note that in a sinusoid of 10-100 μm, the wavelength is equal to 100 μm in the x or y directions but equal to 144 μm in the diagonal direction, which is similar to the diameter of the largest cell considered here. On the contrary, smaller wavelengths, for instance 30 μm, offer several concave spaces that are too small for relaxation of 100 μm cell. The nucleus leaves the convex zones but can stabilize in a metastable equilibrium in an intermediate concave zone.

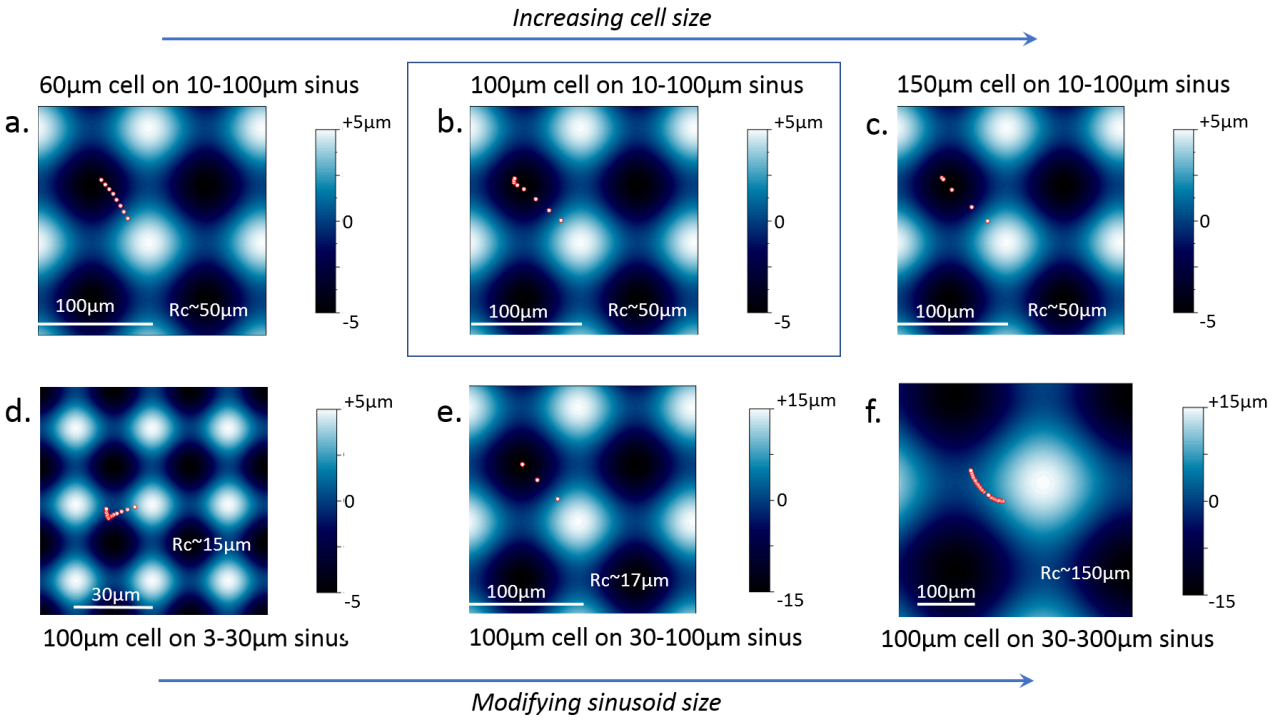

Figure 4: **Influence of cell and sinus sizes on cell trajectories.** Trajectories of the center of the cell model during migration over various sinusoid substrates. The points composing the trajectories are spaced of the same time step, so large gap between two neighboring points indicates large migration velocity. Migration of (a) 60μm, (b) 100μm and (c) 150μm cells migrating on 10-100μm sinusoid. 100μm cell migrating on (d) 3-30μm, (e) 30-100μm and (f) 30-300μm sinusoids. (b) was chosen as reference. For each sinusoid substrate, the minimum cuvarture radius Rc of concave area is indicated using the formula $L^2/(4*A*pi^2)$ with L, the wavelength and A the 0-to-max amplitude of the sinusoid. The cell model started from the slope of the sinusoid and reached full concave sites (a, b, c, d) or intermediate concave sites (d, f) of center. Normalized to the one in b, the cell model migration velocity is equal to 0.5 in a), 1,8 in c), 0,23 in d), 1,85 in e) and 0,29 in f).

Curvotaxis at small wavelength seems limited. Similarly, long-wave curvotaxis is also limited: large sinusoids are almost flat surfaces that offers almost no relaxation zone. In addition, our simulations indicate that regardless of cell and sinusoid sizes, the cell model can not migrate a distance greater than the sinusoid wavelength which represents the spatial scale of the curvotaxis of the model.

The simulated cells tend to stop their migration in the first local minimum of topography they encounter. Only if a cell faces an important deceleration, inertial forces could push it over a local maximum. Conversely, *in vitro* trajectories illustrate the motion of cells from one concave to another (see figure S4.e). *In vitro*, first and foremost cells migrate following a persistent random walk (56), external gradients, such as topography, are only a supplementary perturbation. We simulate the migration of cell subject to a transient directed walk (see 6). Migration is directed diagonally across the substrate, and the cell is left to adapt its position to the topography. The resulting trajectory (see figure 6, and animation S3) features a motion of the cell across multiple convexes before stabilizing in a concave. The cell model is seen to drift away, to the right side of the imposed directed motion. In turn, the nucleus polarization induced migration alters the persistent random walk of the cell. The coordination between the nucleus and the cell barycenter resembles closely experimental evidences (see figure S4.e), that is a systematic offset of the nucleus toward the closest concave region.

We also observe the correlation between the cells trajectory, the nucleus pressure and the substrate topography (see figure 2.b,c). Simulated values of vertical stress on the nucleus are consistent with experimental measurements (57). Additionally, we compute the time evolution cell velocity and the nucleus pressure (see figure 2.c). We draw three main observations from these simulations. (i) Migration is faster on lower curvature gradients (orange and blue cells), namely on more vertical slopes of the substrate. On the contrary, in the middle of concave (yellow cell) or convex (purple cell, at early stages) migration is almost absent. Yet, convex being an unstable equilibrium, a slight offset of the cell position later triggers migration (purple, at later

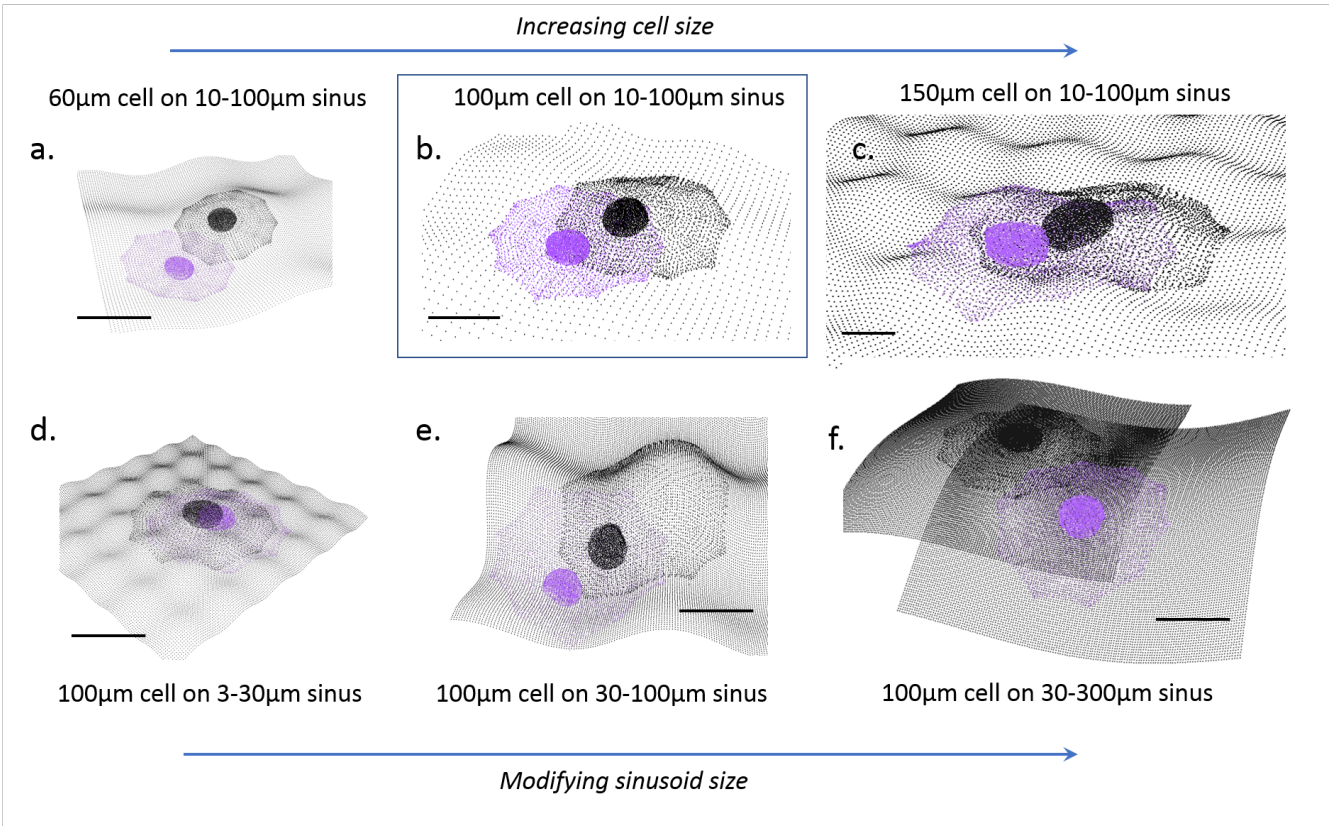

Figure 5: **Influence of cell and sinus sizes on cell shapes.** Beginning (black) and End (purple) of Cell model migration on various sinus substrates. Migration of (a) 60μm, (b) 100μm and (c) 150μm cells migrating on 10-100μm sinusoid. 100μm cell migrating on (d) 3-30μm, (e) 30-100μm and (f) 30-300μm sinusoids. (b) was chosen as reference. Scale bars indicate 40μm

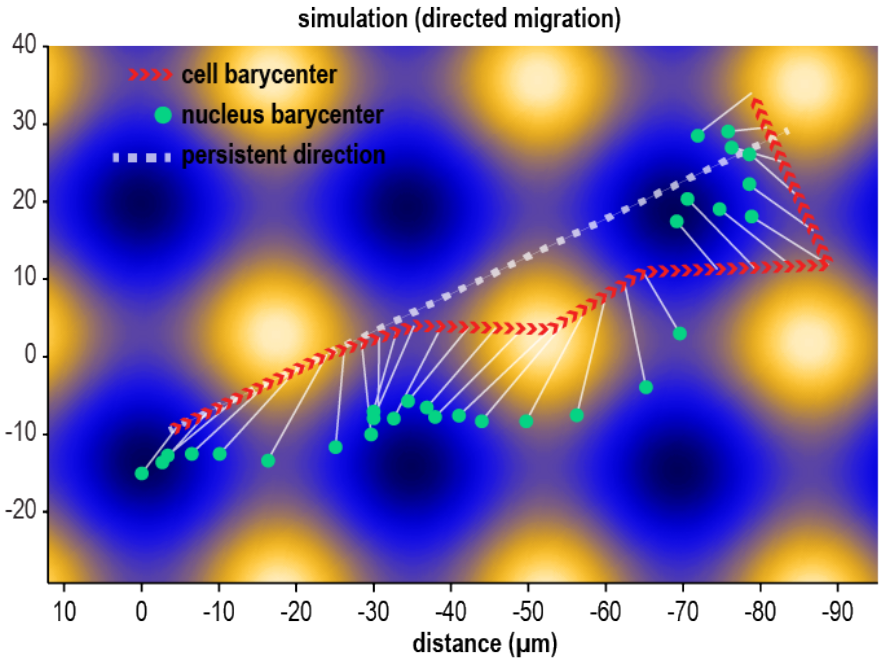

Figure 6: **Directed cell migration.** The cell moves following an imposed direction of migration reproducing a transient stage of a persistent random walk. The direction of persistent motion is indicated by the dashed white line. The red arrowheads show the motion of the cell barycenter, and the green dots the motion of the nucleus barycenter. The white arrows link the position of the cell and its nucleus at a given time. The cell migrates across the substrate mostly following the direction of persistent walk, but finally stabilizes in a concave region. Throughout the migration process the nucleus position itself in more concave regions to find a local minimum of potential energy. Simulation of migration on 10-30μm sinusoid.The animation of this simulation is available in the Supplementary Information (see animation S3).

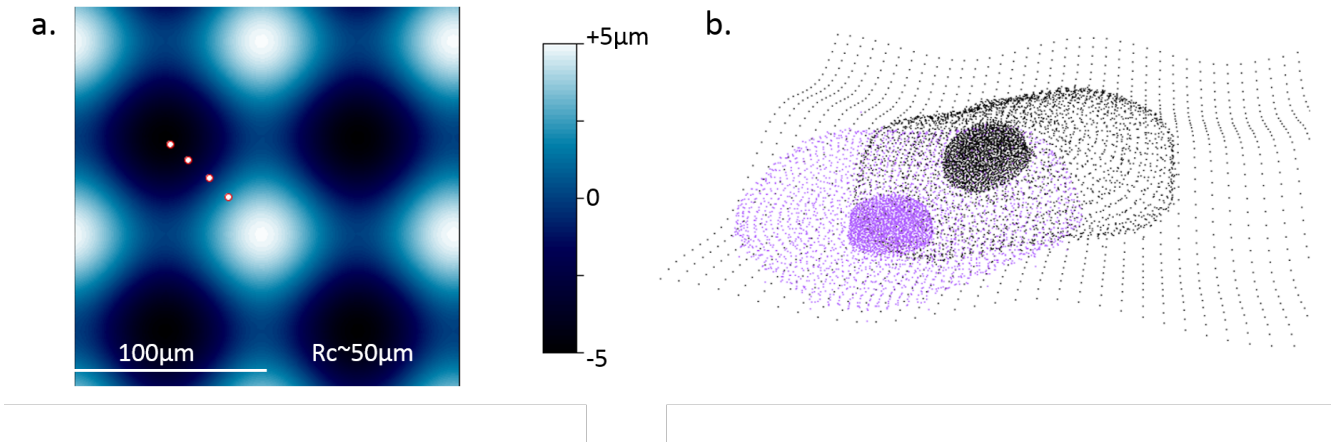

Figure 7: **Cell migration with convex curvature-induced CSK reinforcement**. The number of FAs and stress fibers were doubled after the spreading of the cell model due to experiencing of convex curvature, following in vitro observations of Yevick et al. 2015 (58). Case of the 100μm-spread cell migrating on 10-100μm sinusoid. (a) Trajectory of cell center on sinusoid. (b) cell location at the beginning (black) and at the end of migration (purple)

stages). (ii) An increasing slope, transitioning from concave to convex, induces the cell to slow down, and stopping (purple cell), to change direction (pink cell, midway), or even to turn back (orange and blue cells). (iii) A peak of vertical stress of the nuclei is always a precursor of an acceleration of the cell. The acceleration of the cell is more or less delayed by the cell position of the cell. When the peak stress occurs on curved part (convex) of the substrate (purple cell), the acceleration of the cell is long delayed, while, when the peak stress occurs on a flat part of the sinusoid, the acceleration increases right after (orange, pink, and blue cells).

Yevick et al. observed in 2015 that the convex curvature of the substrate induced the reinforcement of CSK in cultured cells (58). For instance, a convex curvature of 40 μm radius induced a density of FA that was twice that observed on flat substrates. To take into account this phenomenon and analyze its impact on the migratory behavior of the cell, we simulated a reinforcement of the CSK by doubling the number of FAs in the case of cell model adhesion on the slope of a sinusoid of 10-100 μm. This sinusoid has a minimum radius of curvature of approximately 50 μm, close to the 40 μm threshold identified by Yevick et al. (58). Our results indicate that the reinforcement of CSK tends to accelerate cell migration to concave areas by multiplying the speed by 1.2 and making the trajectory much more straight towards the concave center in reducing inertial fluctuations of nuclear displacement (see figure 7). Nonetheless, at the end of migration, after having reached concave zone, and following the same theory, the CSK should relax and the number of FA should decrease to its initial value or to a lower value. In other words, taking into account convex curvature-induced CSK reinforcement in cell migration should lead to the same final adherent state in the concave area via a faster path. Further development in the modeling of dynamic CSK rearrangement and FA formation depending on substrate curvature should be considered in future studies to analyze how cells optimize their CSK to migrate on sinusoid substrates (29).

In presence of drugs deactivating LAMIN-A (nucleus stiffness) and actomyosin contractility (cytoplasmic membrane tension), tested cells by Pieuchot et al. (29) do not exhibit directed migration toward concave regions (see figure S4.b). This agrees with what we observed earlier in cell adhesion simulations (see figure 3.a). Furthermore, when we simulate cell migration with reduced cortical tension (see figure 3.c,d), we indeed observe a significant slow down of cell migration. Conversely, our proposed migration mechanism, as illustrated with these simulations, explains the experimental evidences of a curvature-guided migration mechanism relying on nucleus mechanosensitivity.

To generalize our computational results, curvotaxis is optimized when cell adheres and migrates on sinusoid with a wavelength similar to cell diameter, and a min-to max amplitude equal to the wavelength/10. In that case, the cell model in concave area have a volume which is twice of the one on convex area; the nuclear volume shows the same trend. These changes in cell and nucleus volumes which are direct consequence of substrate topography, are involved in mechanotransduction as reported by Xie (59) and Pieuchot et al. (29). Sinusoid substrates may be so designed in the future to induce stem cell differentiation or on the contrary to maintain their initial phenotype.

CONCLUSION

We have investigated cell migration on substrates with microscopic sinusoid curvature by means of a computational model. We focused on the mechanical features of the migration process, and proposed a simple physical mechanism explaining the trajectories of cell on curved substrates. The parameterized and validated mechanical cell model (28) provided insights, inaccessible experimentally, on the mechanical state of intracellular structures, such as the cytoskeleton, the nucleus, and the cytoplasmic membrane. We have simulated cell adhesion on several location of the sinusoid topography and observed the emergence of a pattern in nucleus behaviour. The nucleus systematically moves such as to find its most relaxed state, that is toward concave parts of the substrate. That internal motion of the nucleus was triggered by a pressure gradient in the cytoskeleton, induced by the asymmetrical underlying topography.

We then proposed that nuclear polarization would promote focal adhesion dynamics and guide cell migration direction. Such mechanism can be seen as an energy efficient process to restore cell equilibrium. We implemented this hypothesis in our computational model, converting nuclear polarization into lamellipodium protrusion and a net spatial jump in cell adhesions position, which simulated cell migration. We have been able to explore how the substrate curvature and the nucleus mechanical state would correlate with the migration patterns, which the model reproduced accurately. We have also shown how the mechanical properties of the intracellular structures contribute to this migration mechanism.

In a nutshell, cell migration on cell-scale curvatures seems highly influenced by the mechanosensitivity of the nucleus, and could be explained almost entirely from a mechanical standpoint. This migration mechanism, guided by nucleus polarization, disrupts the persistent random walk followed by migrating cells. As such, the role of the nucleus as a topographical sensor and mechanical guide should be explored more systematically in other migration modes, at least those involving its polarization (i.e ratchetaxis, topotaxis). The underlying consequences on the mechanical state of the nucleus, chromatin condensation, and therefore gene expression could in turn offer novel control opportunities over cell fate and epigenetics.

AUTHOR CONTRIBUTIONS

Maxime Vassaux, Laurent Pieuchot and Jean-Louis Milan designed the research and analysed the data. Maxime Vassaux and Jean-Louis Milan carried out simulations. Maxime Vassaux wrote the article. Laurent Pieuchot and Jean-Louis Milan edited the article.

ACKNOWLEDGMENTS

The authors would like to thank F. Dubois and his research team for making the LMGC90 software freely available. This work was supported by a grant from the French Research National Agency (ANR-12-BSV5-0010).

SUPPLEMENTARY MATERIAL

An online supplement to this article can be found by visiting BJ Online at http://www.biophysj.org.

REFERENCES

1. Vogel, V., and M. Sheetz, 2006. Local force and geometry sensing regulate cell functions. *Nature Reviews Molecular Cell Biology* 7:265–275. http://www.nature.com/nrm/journal/v7/n4/abs/nrm1890.html.

2. Isenberg, B. C., P. A. DiMilla, M. Walker, S. Kim, and J. Y. Wong, 2009. Vascular Smooth Muscle Cell Durotaxis Depends on Substrate Stiffness Gradient Strength. *Biophysical Journal* 97:1313–1322. http://www.sciencedirect.com/science/article/pii/S0006349509011540.

3. Kim, D.-H., P. P. Provenzano, C. L. Smith, and A. Levchenko, 2012. Matrix nanotopography as a regulator of cell function. *The Journal of Cell Biology* 197:351–360. http://jcb.rupress.org/content/197/3/351.

4. Bershadsky, A., N. Q. Balaban, and B. Geiger, 2003. Adhesion-Dependent Cell Mechanosensitivity. *Annual Review of Cell and Developmental Biology* 19:677–695. http://dx.doi.org/10.1146/annurev.cellbio.19.111301.153011.

5. Vogel, V., and M. P. Sheetz, 2009. Cell fate regulation by coupling mechanical cycles to biochemical signaling pathways. *Current Opinion in Cell Biology* 21:38–46. http://www.sciencedirect.com/science/article/pii/S0955067409000040.

6. Chelberg, M. K., E. C. Tsilibary, A. R. Hauser, and J. B. McCarthy, 1989. Type IV Collagen-mediated Melanoma Cell Adhesion and Migration: Involvement of Multiple, Distinct Domains of the Collagen Molecule. *Cancer Research* 49:4796–4802. http://cancerres.aacrjournals.org/content/49/17/4796.

7. Tan, J. L., J. Tien, D. M. Pirone, D. S. Gray, K. Bhadriraju, and C. S. Chen, 2003. Cells lying on a bed of microneedles: An approach to isolate mechanical force. *Proceedings of the National Academy of Sciences* 100:1484–1489. http://www.pnas.org/content/100/4/1484.

8. Thakar, R. G., Q. Cheng, S. Patel, J. Chu, M. Nasir, D. Liepmann, K. Komvopoulos, and S. Li, 2009. Cell-Shape Regulation of Smooth Muscle Cell Proliferation. *Biophysical Journal* 96:3423–3432. http://www.sciencedirect.com/science/article/pii/S0006349509004883.

9. Fernandez, P., M. Maier, M. Lindauer, C. Kuffer, Z. Storchova, and A. R. Bausch, 2011. Mitotic Spindle Orients Perpendicular to the Forces Imposed by Dynamic Shear. *PLOS ONE* 6:e28965. https://journals.plos.org/plosone/article?id=10.1371/journal.pone.0028965.

10. Grespan, E., G. G. Giobbe, F. Badique, K. Anselme, J. Rühe, and N. Elvassore, 2018. Effect of geometrical constraints on human pluripotent stem cell nuclei in pluripotency and differentiation. *Integrative Biology* 10:278–289. https://pubs.rsc.org/en/content/articlelanding/2018/ib/c7ib00194k.

11. Chen, C. S., M. Mrksich, S. Huang, G. M. Whitesides, and D. E. Ingber, 1997. Geometric control of cell life and death. *Science* 276:1425–1428.

12. Théry, M., V. Racine, A. Pépin, M. Piel, Y. Chen, J.-B. Sibarita, and M. Bornens, 2005. The extracellular matrix guides the orientation of the cell division axis. *Nature Cell Biology* 7:947–953. http://www.nature.com/ncb/journal/v7/n10/abs/ncb1307.html.

13. Bigerelle, M., S. Giljean, and K. Anselme, 2011. Existence of a typical threshold in the response of human mesenchymal stem cells to a peak and valley topography. *Acta Biomaterialia* 7:3302–3311. http://www.sciencedirect.com/science/article/pii/S1742706111002066.

14. Devreotes, P., and C. Janetopoulos, 2003. Eukaryotic Chemotaxis: Distinctions between Directional Sensing and Polarization. *Journal of Biological Chemistry* 278:20445–20448. http://www.jbc.org/content/278/23/20445.

15. Lo, C.-M., H.-B. Wang, M. Dembo, and Y.-l. Wang, 2000. Cell Movement Is Guided by the Rigidity of the Substrate. *Biophysical Journal* 79:144–152. http://www.sciencedirect.com/science/article/pii/S0006349500762795.

16. Park, J., D.-H. Kim, and A. Levchenko, 2018. Topotaxis: A New Mechanism of Directed Cell Migration in Topographic ECM Gradients. *Biophysical Journal* 114:1257–1263. http://www.sciencedirect.com/science/article/pii/S0006349518301516.

17. Jiang, X., D. A. Bruzewicz, A. P. Wong, M. Piel, and G. M. Whitesides, 2005. Directing cell migration with asymmetric micropatterns. *Proceedings of the National Academy of Sciences* 102:975–978. http://www.pnas.org/content/102/4/975.

18. Comelles, J., D. Caballero, R. Voituriez, V. Hortigüela, V. Wollrab, A. Godeau, J. Samitier, E. Martínez, and D. Riveline, 2014. Cells as Active Particles in Asymmetric Potentials: Motility under External Gradients. *Biophysical Journal* 107:1513–1522. http://www.sciencedirect.com/science/article/pii/S0006349514008054.

19. Caballero, D., J. Comelles, M. Piel, R. Voituriez, and D. Riveline, 2015. Ratchetaxis: Long-Range Directed Cell Migration by Local Cues. *Trends in Cell Biology* 25:815–827. http://www.sciencedirect.com/science/article/pii/S0962892415001968.

20. Park, J. Y., D. H. Lee, E. J. Lee, and S.-H. Lee, 2009. Study of cellular behaviors on concave and convex microstructures fabricated from elastic PDMS membranes. *Lab on a Chip* 9:2043–2049. http://pubs.rsc.org/en/content/articlelanding/2009/lc/b820955c.

21. Song, K. H., S. J. Park, D. S. Kim, and J. Doh, 2015. Sinusoidal wavy surfaces for curvature-guided migration of T lymphocytes. *Biomaterials* 51:151–160.

22. Werner, M., S. B. G. Blanquer, S. P. Haimi, G. Korus, J. W. C. Dunlop, G. N. Duda, D. W. Grijpma, and A. Petersen, 2017. Cell Migration: Surface Curvature Differentially Regulates Stem Cell Migration and Differentiation via Altered Attachment Morphology and Nuclear Deformation (Adv. Sci. 2/2017). *Advanced Science* 4. https://onlinelibrary.wiley.com/doi/abs/10.1002/advs.201770007.

23. Bade, N. D., T. Xu, R. D. Kamien, R. K. Assoian, and K. J. Stebe, 2018. Gaussian Curvature Directs Stress Fiber Orientation and Cell Migration. *Biophysical Journal* 114:1467–1476. http://www.sciencedirect.com/science/article/pii/S0006349518302017.

24. Friedl, P., K. Wolf, and J. Lammerding, 2011. Nuclear mechanics during cell migration. *Current Opinion in Cell Biology* 23:55–64. http://www.sciencedirect.com/science/article/pii/S0955067410001869.

25. Badique, F., D. R. Stamov, P. M. Davidson, M. Veuillet, G. Reiter, J.-N. Freund, C. M. Franz, and K. Anselme, 2013. Directing nuclear deformation on micropillared surfaces by substrate geometry and cytoskeleton organization. *Biomaterials* 34:2991–3001. http://www.sciencedirect.com/science/article/pii/S0142961213000343.

26. Cho, S., J. Irianto, and D. E. Discher, 2017. Mechanosensing by the nucleus: From pathways to scaling relationships. *J Cell Biol* 216:305–315. http://jcb.rupress.org/content/216/2/305.

27. Rosso, G., I. Liashkovich, and V. Shahin, 2018. In Situ Investigation of Interrelationships Between Morphology and Biomechanics of Endothelial and Glial Cells and their Nuclei. *Advanced Science* 0:1801638. https://onlinelibrary.wiley.com/doi/abs/10.1002/advs.201801638.

28. Vassaux, M., and J. L. Milan, 2017. Stem cell mechanical behaviour modelling: substrate's curvature influence during adhesion. *Biomechanics and Modeling in Mechanobiology* 1–14. https://link.springer.com/article/10.1007/s10237-017-0888-4.

29. Pieuchot, L., J. Marteau, A. Guignandon, T. D. Santos, I. Brigaud, P.-F. Chauvy, T. Cloatre, A. Ponche, T. Petithory, P. Rougerie, M. Vassaux, J.-L. Milan, N. T. Wakhloo, A. Spangenberg, M. Bigerelle, and K. Anselme, 2018. Curvotaxis directs cell migration through cell-scale curvature landscapes. *Nature Communications* 9:3995. https://www.nature.com/articles/s41467-018-06494-6.

30. Cheng, B., M. Lin, G. Huang, Y. Li, B. Ji, G. M. Genin, V. S. Deshpande, T. J. Lu, and F. Xu, 2017. Cellular mechanosensing of the biophysical microenvironment: A review of mathematical models of biophysical regulation of cell responses. *Physics of Life Reviews* 22-23:88–119. http://www.sciencedirect.com/science/article/pii/S1571064517300878.

31. Mak, M., T. Kim, M. H. Zaman, and R. D. Kamm, 2015. Multiscale mechanobiology: computational models for integrating molecules to multicellular systems. *Integrative Biology* 7:1093–1108. https://pubs.rsc.org/en/content/articlelanding/2015/ib/c5ib00043b.

32. Graner, F., and J. A. Glazier, 1992. Simulation of biological cell sorting using a two-dimensional extended Potts model. *Physical Review Letters* 69:2013–2016. https://link.aps.org/doi/10.1103/PhysRevLett.69.2013.

33. Allena, R., M. Scianna, and L. Preziosi, 2016. A Cellular Potts Model of single cell migration in presence of durotaxis. *Mathematical Biosciences* 275:57–70. http://www.sciencedirect.com/science/article/pii/S0025556416000420.

34. Rens, E. G., and R. M. H. Merks, 2017. Cell Contractility Facilitates Alignment of Cells and Tissues to Static Uniaxial Stretch. *Biophysical Journal* 112:755–766. http://www.cell.com/biophysj/abstract/S0006-3495(16)34287-4.

35. Prost, J., J.-F. Chauwin, L. Peliti, and A. Ajdari, 1994. Asymmetric pumping of particles. *Physical Review Letters* 72:2652–2655. https://link.aps.org/doi/10.1103/PhysRevLett.72.2652.

36. Kim, M.-C., C. Kim, L. Wood, D. Neal, R. D. Kamm, and H. H. Asada, 2012. Integrating focal adhesion dynamics, cytoskeleton remodeling, and actin motor activity for predicting cell migration on 3D curved surfaces of the extracellular matrix. *Integrative Biology* 4:1386–1397.

37. Fang, Y., and K. W. C. Lai, 2016. Modeling the mechanics of cells in the cell-spreading process driven by traction forces. *Phys. Rev. E* 93:042404. http://link.aps.org/doi/10.1103/PhysRevE.93.042404.

38. Fang, Y., Q. Gao, R. Yang, and K. W. C. Lai, 2017. Computational Modeling of Cell Adhesion under the Effect of Substrate Stiffness. *IEEE Transactions on Nanotechnology* PP:1–1.

39. Dubois, F., and M. Jean, 2006. The non smooth contact dynamic method: recent LMGC90 software developments and application. *In* P. W. P. Dr, and U. N. P. Dr, editors, Analysis and Simulation of Contact Problems, Springer Berlin Heidelberg, number 27 in Lecture Notes in Applied and Computational Mechanics, 375–378.

40. Milan, J.-L., S. Wendling-Mansuy, M. Jean, and P. Chabrand, 2007. Divided medium-based model for analyzing the dynamic reorganization of the cytoskeleton during cell deformation. *Biomechanics and modeling in mechanobiology* 6:373–390.

41. Milan, J., S. Lavenus, P. Pilet, G. Louarn, S. Wendling, D. Heymann, P. Layrolle, and P. Chabrand, 2013. Computational model combined with in vitro experiments to analyse mechanotransduction during mesenchymal stem cell adhesion. *European cells & materials* 25:97.

42. Milan, J.-L., I. Manifacier, K. M. Beussman, S. J. Han, N. J. Sniadecki, I. About, and P. Chabrand, 2016. In silico CDM model sheds light on force transmission in cell from focal adhesions to nucleus. *Journal of Biomechanics* http://linkinghub.elsevier.com/retrieve/pii/S0021929016306297.

43. Knotts, T. A., N. Rathore, D. C. Schwartz, and J. J. de Pablo, 2007. A coarse grain model for DNA. *The Journal of Chemical Physics* 126:084901. https://aip.scitation.org/doi/abs/10.1063/1.2431804.

44. Tozzini, V., 2005. Coarse-grained models for proteins. *Current Opinion in Structural Biology* 15:144–150. http://www.sciencedirect.com/science/article/pii/S0959440X05000515.

45. Cañadas, P., V. M. Laurent, C. Oddou, D. Isabey, and S. Wendling, 2002. A Cellular Tensegrity Model to Analyse the Structural Viscoelasticity of the Cytoskeleton. *Journal of Theoretical Biology* 218:155–173. http://linkinghub.elsevier.com/retrieve/pii/S002251930293064X.

46. Chélin, Y., K. Azzag, P. Cañadas, J. Averseng, S. Baghdiguian, and B. Maurin, 2013. Simulation of cellular packing in non-proliferative epithelia. *Journal of Biomechanics* 46:1075–1080. http://www.sciencedirect.com/science/article/pii/S0021929013000560.

47. Maniotis, A. J., C. S. Chen, and D. E. Ingber, 1997. Demonstration of mechanical connections between integrins, cytoskeletal filaments, and nucleoplasm that stabilize nuclear structure. *Proceedings of the National Academy of Sciences* 94:849–854.

48. Bansod, Y. D., T. Matsumoto, K. Nagayama, and J. Bursa, 2018. A Finite Element Bendo-Tensegrity Model of Eukaryotic Cell. *Journal of Biomechanical Engineering* 140:101001–101001–9. http://dx.doi.org/10.1115/1.4040246.

49. Rabineau, M., F. Flick, E. Mathieu, A. Tu, B. Senger, J.-C. Voegel, P. Lavalle, P. Schaaf, J.-N. Freund, Y. Haikel, and D. Vautier, 2015. Cell guidance into quiescent state through chromatin remodeling induced by elastic modulus of substrate. *Biomaterials* 37:144–155. http://www.sciencedirect.com/science/article/pii/S0142961214010709.

50. Elosegui-Artola, A., I. Andreu, A. E. M. Beedle, A. Lezamiz, M. Uroz, A. J. Kosmalska, R. Oria, J. Z. Kechagia, P. Rico-Lastres, A.-L. L. Roux, C. M. Shanahan, X. Trepat, D. Navajas, S. Garcia-Manyes, and P. Roca-Cusachs, 2017. Force Triggers YAP Nuclear Entry by Regulating Transport across Nuclear Pores. *Cell* 171:1397–1410.e14. https://www.cell.com/cell/abstract/S0092-8674(17)31192-3.

51. Almonacid, M., W. W. Ahmed, M. Bussonnier, P. Mailly, T. Betz, R. Voituriez, N. S. Gov, and M.-H. Verlhac, 2015. Active diffusion positions the nucleus in mouse oocytes. *Nature Cell Biology* 17:470–479. http://www.nature.com/ncb/journal/v17/n4/abs/ncb3131.html.

52. Azoury, J., K. W. Lee, V. Georget, P. Hikal, and M.-H. Verlhac, 2011. Symmetry breaking in mouse oocytes requires transient F-actin meshwork destabilization. *Development* 138:2903–2908. http://dev.biologists.org/content/138/14/2903.

53. Laan, L., N. Pavin, J. Husson, G. Romet-Lemonne, M. van Duijn, M. P. López, R. D. Vale, F. Jülicher, S. L. Reck-Peterson, and M. Dogterom, 2012. Cortical Dynein Controls Microtubule Dynamics to Generate Pulling Forces that Position Microtubule Asters. *Cell* 148:502–514. http://www.cell.com/cell/abstract/S0092-8674(12)00013-X.

54. Ma, R., L. Laan, M. Dogterom, N. Pavin, and F. Jülicher, 2014. General theory for the mechanics of confined microtubule asters. *New Journal of Physics* 16:013018. http://stacks.iop.org/1367-2630/16/i=1/a=013018.

55. Raucher, D., and M. P. Sheetz, 2000. Cell Spreading and Lamellipodial Extension Rate Is Regulated by Membrane Tension. *J Cell Biol* 148:127–136. http://jcb.rupress.org/content/148/1/127.

56. Wu, P.-H., A. Giri, S. X. Sun, and D. Wirtz, 2014. Three-dimensional cell migration does not follow a random walk. *Proceedings of the National Academy of Sciences* 111:3949–3954. http://www.pnas.org/content/111/11/3949.

57. Lammerding, J., 2011. Mechanics of the Nucleus. *In* Comprehensive Physiology, American Cancer Society, 783–807. https://onlinelibrary.wiley.com/doi/abs/10.1002/cphy.c100038.

58. Yevick HG, B. I. S. P., Duclos G, 2015. Architecture and migration of an epithelium on a cylindrical wire. *Proc Natl Acad Sci U S A* 10:5944–9. http://pubs.rsc.org/en/content/articlelanding/2014/sm/c4sm90028f.

59. Xie, Y. Y. . J. H. ., K., 2018. Controlling Cellular Volume via Mechanical and Physical Properties of Substrate. *Biophysical journal* 3:675–87. http://pubs.rsc.org/en/content/articlelanding/2014/sm/c4sm90028f.